Intermetallic growth in gold ball bonds aged at 175°C: comparison between two 4N wires of different chemistry

C.D. Breach[1], F.W. Wulff[2]

[1] #10-04, 166 Lentor Loop, Singapore 789097, email: cbreach@physics.org
[2] Materials & Applications Centre, Kulicke & Soffa Pte. Ltd., #04-05 TECHPlace II, Ang Mo Kio Ave 5, Singapore 569871, email: fwwulff@gmail.com

Abstract

Gold wires of different chemistry (denoted as Types A and B) are ballbonded on identical metallization and isothermally aged at 175°C. In both wire types the same intermetallic compounds Au_4Al and Au_8Al_3 grow with parabolic time dependence as long as there is a supply of Al from the bondpad. After Al is completely reacted, composition of intermetallics in Type A wire remains unchanged but in Type B wire, the Au_8Al_3 compound undergoes a phase transformation into a second layer of Au_4Al. The phase transformation does not affect mechanical reliability of the ballbonds. Intermetallic growth kinetics, growth sequence and the possible origins of the phase transformation are discussed.

Keywords: Gold ballbond, intermetallics, intermetallic growth, reliability

1 Introduction

Thermosonic ballbonding is a solid-state metallurgical joining process used in the assembly of microelectronics packages to weld gold or copper balls formed at the end of a wire (using an electric arc, see ref [1]) to metal bondpads on the surface of Si chips. The wire forms a mechanically reliable electrical connection between chip and substrate. The term 'thermosonic' is used because the process uses moderate heating of the chips and ultrasonic vibrations to form the weld between the wire and the most common bondpad metals, which are aluminium alloys typically containing silicon, copper or a combination of the two elements. Device pre-heating is usually in the range of 170-250°C depending on the package type and is typically at the lower end for chips on polymeric substrates and at the higher end for chips attached to metal substrates (leadframes). Gold ballbonding is currently one of the major interconnect processes in microelectronics packaging and although copper wire ballbonding may eventually dominate in consumer applications, the use of gold wire is expected for some considerable time in high reliability applications such as automotive and aerospace. With gold ballbonding, the bond results from formation of gold – aluminium intermetallics that are typically 0.5µm thick when bonded to 1µm thick bondpad metallization. Stronger welds result from a larger area of intermetallics at the interface (called intermetallic coverage or IMC for short) and together with neckpull and shear strength, IMC is one of the responses that the wirebond process engineer aims to maximize to achieve a robust process.

After ballbonding, semiconductor chips undergo further processing. Wires are encapsulated with viscous epoxy based moulding compounds that are typically cured at 175°C for several hours and provide the chip and wires with chemical and mechanical protection. Assembled packages may undergo further processing such mounting to other substrates using reflow soldering, which typically exposes the package to two minutes above 220°C and a peak temperature of 260°C. The elevated temperatures reached during post-wirebond processing cause growth of IMC into thicker layers. Further growth of intermetallics during HTS is usually limited to gold rich compounds because of the plentiful supply of gold from the wire. Some studies suggest that in general only three compounds occur and in proportions that depend on time and wire chemistry [2], while others suggest that all compounds grow and are seen in ballbonds [3,4]. Like most intermetallics, gold – aluminium intermetallics are brittle. If intermetallics grow uniformly across the ballbond the electrical connection should remain robust but if growth is non-uniform, stresses evolved as a result of interdiffusion cannot be relaxed and can lead to fracture. However, with optimised ballbonding, encapsulation and solder reflow process parameters, as well as compatible wire, bondpad and encapsulant materials, intermetallic growth

should occur relatively uniformly resulting in a reliable microelectronics package.

Selection of gold bonding wires usually starts with optimizing the bonding process on mechanical (non-functional) devices without epoxy encapsulation. Isothermal ageing of the devices at 175°C may be performed for extended periods of time up to 1000 hours (usually in air), or more if required, in order to determine the mechanical robustness of the ballbonds as intermetallics grow. This test is normally referred to as high temperature storage (HTS) test. Wires are often considered to pass the intermetallic growth tests if the mechanical strength exceeds a predefined threshold and if there are no lifted ball failures. There may be a similar process of encapsulant selection by repeating the HTS test with the best-performing wires from the bare device test and selecting encapsulants that give the best results. Encapsulant-wire compatibility may be judged on the uniformity of intermetallic growth as well as wire pull strength after removal of the encapsulant with fuming nitric acid [5].

The ability of wire chemistry to influence intermetallic growth and stability in gold ballbonds generally disregarded and almost all studies of intermetallic growth discuss binary intermetallics. Some studies consider the effects of wire chemistry, for example Blish et al [6], concluding that there is an impact on reliability. There is however an overall lack of attention to wire chemistry, probably due to the fact that regardless of wire type, the same intermetallics appear to grow in the same sequence in ballbonds, at least as far as EDX (the most commonly used tool for analysing chemical composition) can tell [7-9]. In addition, there is the perception that dopants present in such small concentrations cannot affect intermetallics, despite the fact that they are responsible for significant property changes in wires [10, 11]. Impurities at parts-per-million concentrations are also known to affect intermetallic growth [12]. In addition, the influence of bondpad elements such as Cu and Si on intermetallic structure and properties, which are present in much larger amounts than dopants, also receives little attention. The few studies that are available can be contradictory. For example, with regard to elements found in bondpads an early study by Philofsky suggests that Si forms Au-Si-Al compounds [13] while Noolu et al conclude that Cu in the bondpad has no effect on intermetallic type or growth [14]. However, an interesting phenomenon in 4N wires that suggests wire chemistry may influence the type of intermetallic in ballbonds is the observation that at long ageing times Au_8Al_3 transforms into another layer of Au_4Al [15]. This article presents experimental data on the growth of the new layer of Au_4Al and proposes a mechanism that may be responsible for the phase change.

2 Experimental details

Two experimental 4N wire types denoted as Type A and Type B, each 20µm in diameter were bonded on BGA devices with 1µm thick Al-0.5%Cu-1%Si metallization at 50µm with a bond pad opening of 45µm using a K&S Maxµm ball bonder. Identical devices and substrates were used. Prior to bonding, devices were plasma cleaned in argon. The elements contained in each wire are not explicitly given for proprietary reasons but are labelled A-D and summarized in Table 1. Bonded ball height was 8±2µm. Bond site temperature was set at 170°C. Optimum 1st bond parameters were obtained using response surface methodology with free air ball (FAB) size, CV (contact velocity), power, time and force as the variables and a population size of 30 balls for each type of device. Statistical software was used to analyze data and optimum parameters were confirmed by bonding 60 balls and measuring the shear and pull values using a Dage 4000 series wirebond & neckpull/shear tester with a speed of 300µm per second. Procedures for measuring intermetallic coverage are given elsewhere [2].

High temperature storage (HTS) testing was performed by placing bonded devices in a fan assisted oven at 175°C at various time intervals. Devices were aged in air. Intermetallic thickness was measured from secondary electron SEM images of cross-sectioned devices. Measurements were made at the centre of ballbonds where growth is relatively uniform. The chemical composition of phases was measured with a Leo 1450VP SEM, equipped with an Oxford Instruments Inca EDX system. Etching of samples with aqua-regia was performed to examine the morphology of individual phases. Backscattered electron imaging was also used to distinguish intermetallics by atomic number contrast.

Table 1

Main dopants and alloy elements present in the wires and bondpad

Material	Wire dopants concentration (ppm by weight)				Bondpad elements (% by weight)	
	A	B	C	D	Si	Cu
Wire A	50	40	–	–	–	–
Wire B	30	10	10	30	–	–
Bondpad	–	–	–	–	1	0.5

Figure 1

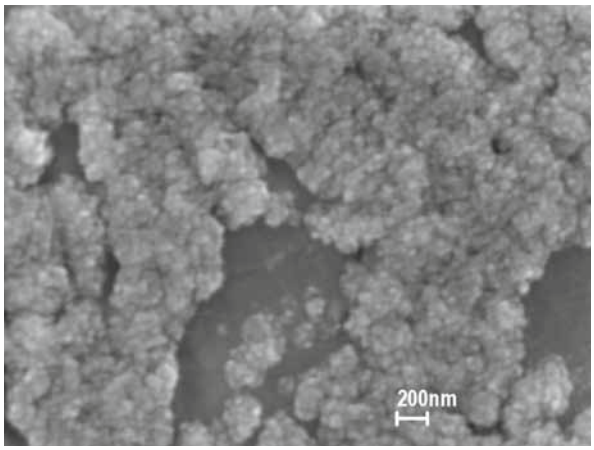

SE-SEM image of as bonded intermetallic morphology showing nano-sized spherical particulate structure

Figure 2

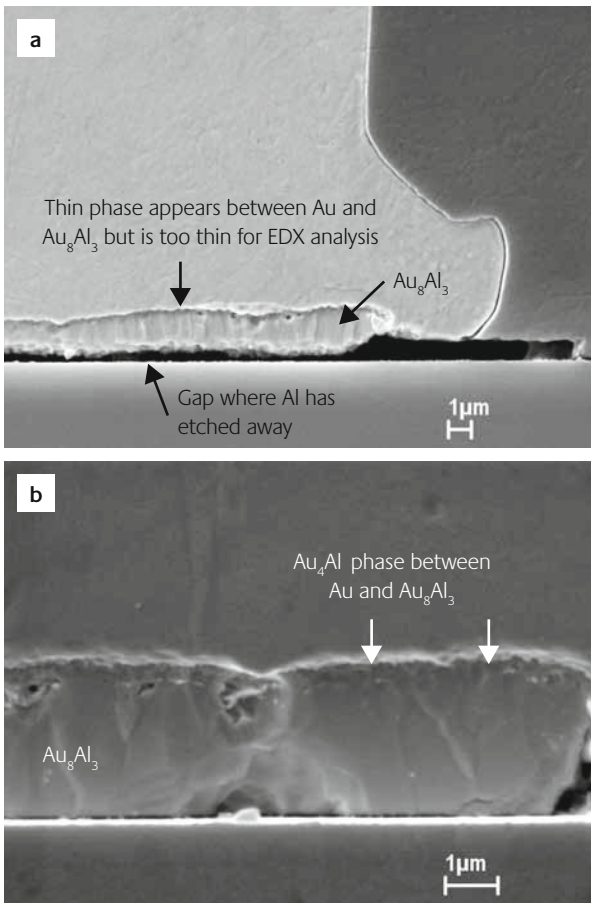

Typical SEM, SE images of a ballbond of Wire Type A after isothermal ageing at 175°C and representative of Wire Type B. (a) 2 hours ageing showing thick layer of Au_8Al_3. Gap is due to etching away of unconsumed aluminium. (b) 20 hours ageing at 175°C. A thin upper layer previously assumed to be $Au_4Al(1)$ is seen together with a thick lower layer of Au_8Al_3. White arrows show interfacial flakes

3 Results

3.1 Intermetallic growth and microstructure

The weld between gold wire and aluminium bondpads is due to the formation of an intermetallic phase consisting of discrete nanometre sized spherical particles, shown in Fig 1. There are spaces between the coverage where the ball does not weld to the bondpad. During ageing, coverage develops into well-defined intermetallic phases and thermodynamics predicts that the first phase is Au_8Al_3 because it has the most negative effective heat of formation [16] (see Table 2). After 2 hours at 175°C Fig. 2(a) shows a very thick Au_8Al_3 phase, as expected. Another phase, too thin for analysis by EDX, is visible between Au_8Al_3 and the gold ball. Thin film studies [17] suggest the phase is Au_2Al but with an infinite supply of Au and a finite supply of Al it may also be Au_4Al, which has the next most negative heat of formation. Further intermetallic growth occurs as long as a supply of Al is available and Au_4Al later forms a distinct and thin layer between Au and Au_8Al_3. After 20 hours, when the supply of Al has more or less exhausted, Au_4Al is clearly visible in Fig. 2(b) and is roughly 0.5µm thick. The intermetallics shown in Fig 2 are formed with A wire but are equally representative of B wire. In both wire types, intermetallic growth is similar to that reported in many studies [7-9] and wire chemistry does not appear to affect the type of compounds or the sequence in which they are formed as long as gold and aluminium from the wire and bondpad respectively, are available to feed the reaction.

When intermetallic reactions consume all bondpad aluminium, further growth or formation of compounds should stop. Therefore, further ageing beyond the time at which the last Al is consumed ought not to result in any chemical changes to the compounds. Examination of Fig. 3(a) and Fig. 3(b) show that intermetallics with Type A wire are unchanged. However, after long term ageing of Type B wire a second layer of Au_4Al forms between the first layer of Au_4Al and Au_8Al_3 as SEM images in Fig. 3(c) and Fig. 3(d) clearly show. The second Au_4Al layer seems to form at the expense of Au_8Al_3. The first layer of Au_4Al has fine columnar grains (roughly 0.25µm wide), which suggests a very high density of nucleation points and strongly directional growth while the second Au_4Al layer has the same coarse grain size as Au_8Al_3 (roughly 1-3µm wide). However, Au_8Al_3 is still present at the peripheral regions of the ball with minor

Table 2

Parabolic growth rates measured for the total compound thickness from the graphs in Fig. 1

Wire Type	Growth Rate k_p ($m^2s^{-1} \times 10^{-16}$)
A	1.32
B	0.35

Figure 3

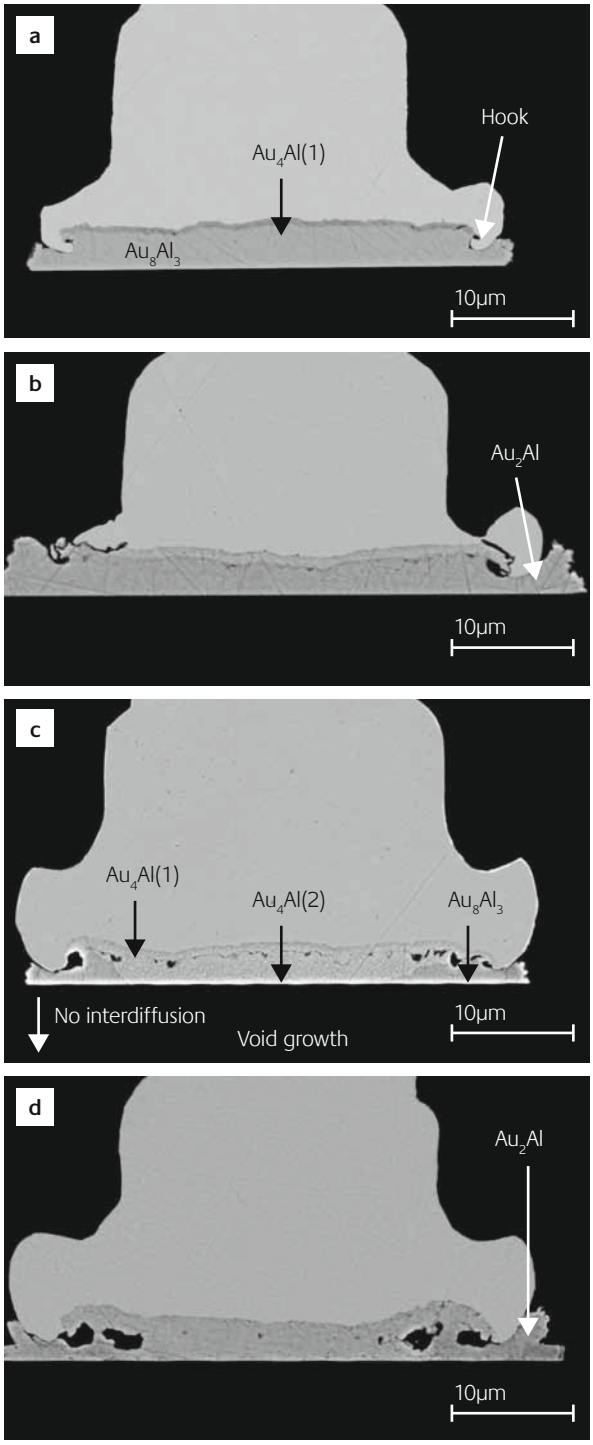

Wire Type A, 20µm diameter. BSE-SEM images of unetched cross-sections. (a) 96 hours at 175°C (b) 1000 hours at 175°C. BSE-SEM images of unetched cross-sections of Wire Type B, 20µm diameter (c) 96 hours at 175°C (d) 500 hours at 175°C. Note that there appears to be a layer of different contrast between the gold ball and $Au_4Al(1)$

amounts of Au_2Al visible at the outer edge of the ballbond. Voids are present between the Au_4Al layers and at the ball periphery. The peripheral voids enlarge inward towards the centre of the ball after ageing to 500 hrs. A series of images of aged gold ballbonds in Fig. 4 shows the gradual transformation of Au_8Al_3 to Au_4Al.

Figure 4

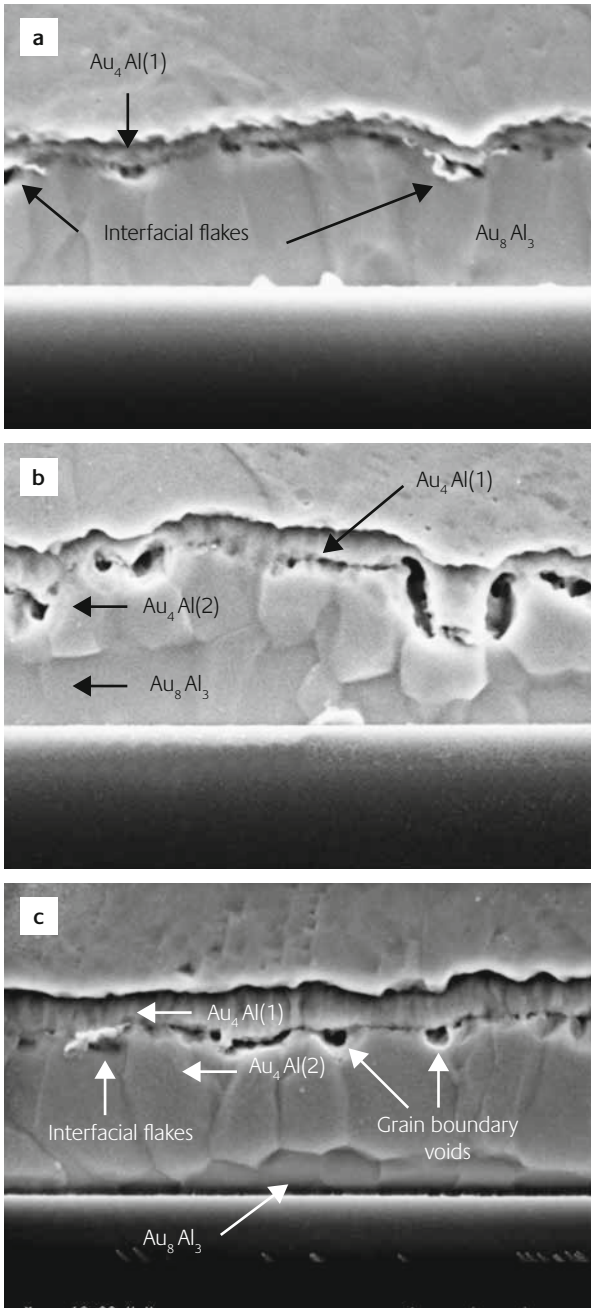

SEM images of etched cross-sections of Type B wire after isothermal ageing at 175°C showing the gradual transformation of Au_8Al_3 → Au_4Al: (a) 96 hrs (b) 200 hrs (c) 500 hrs. Images taken from [4]

An intermetallic phase grows around the sides of the balls (Fig. 5(a)) and EDX analysis shows this phase is Au_2Al. The surface of Au_2Al in contact with air consists of discrete contacting spherical particles, different from the bulk or internal structure of the Au_2Al that can be seen from cross-sections (see Fig. 3). Examination of lifted balls (taken from another reliability study with different wire materials) in Fig. 5(b) shows the morphology of the Au_2Al within the ballbond is columnar, growing around the gold ball and towards the ball edge, not vertically into the gold ball. The very smooth appearance of the columnar intermetallics i.e.

Figure 5

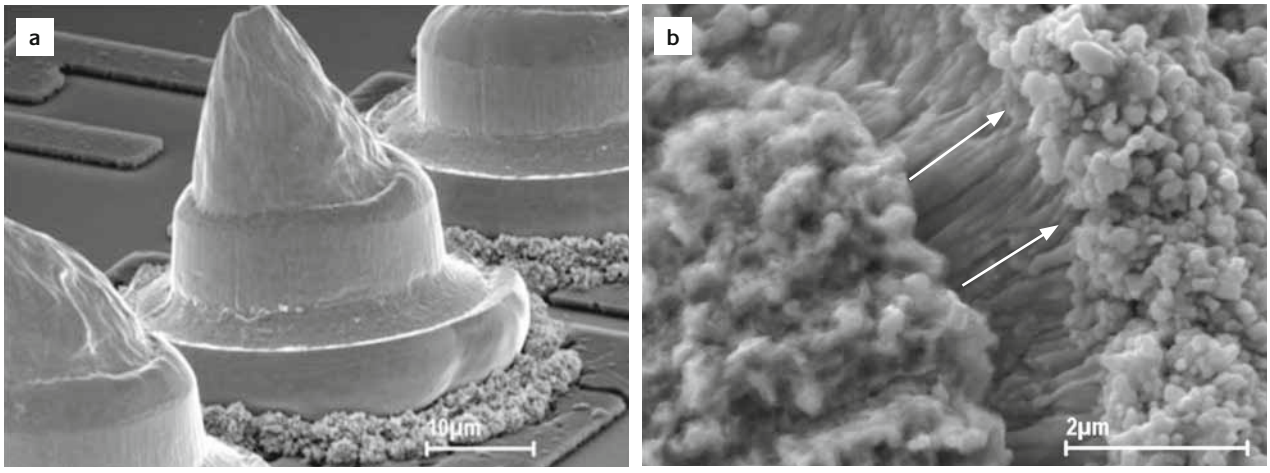

SE-SEM images of (a) ballbond showing growth of the Au_2Al compound at the outside of the ball (b) close-up Au_2Al showing columnar growth directed outwards and around the gold ball

the absence of any features that indicate yield and deformation, suggests there is little or no true contact between the gold ball and Au_2Al. At longer ageing times the enlargement of the voids is concurrent with further growth of Au_2Al. Comparing Fig. 5 with Fig. 4 shows a hook shaped region of the Au ball that appears to be in mechanical contact with the intermetallic and yet Au_2Al grows around rather than into the hook. Voids appear at the ballbond periphery in the period 20-50hrs, enlarge with time, and generally occur in the region under the ball where the ceramic capillary induces the highest stresses during deformation. This is also the region where ball hardness in as-bonded balls is often higher than at other locations due to work hardening [18].

In etched microstructures a flake-shaped phase is sometimes observed at the Au_4Al - Au_8Al_3 interface, which is shown in Fig. 4. The flaky, angular geometry of the material makes it difficult to chemically analyze due to the size of the phase relative to the electron beam. However, the angular appearance of the flakes suggests a hard, brittle phase, possibly an oxide that has grown during ageing. The origin of a flake shaped phase between intermetallics is difficult to determine. The flakes are not visible in as-polished specimens and only appear after etching, and are therefore insoluble, emerging as the surrounding intermetallics are etched away. If the flakes are some form of oxide, they may be due to oxidation of the intermetallic phases because the ballbonded devices are un-encapsulated and air and contaminants (possibly from the plastic substrate), may penetrate underneath the ball.

3.2 Intermetallic growth kinetics and mechanical strength

The graphs in Fig. 6 show intermetallic thickness measured at the centre of the ballbonds as a function of the square root of time. Three parameters are plotted. The thickness of Au_8Al_3 and Au_4Al are shown when the compound thickness is

Figure 6

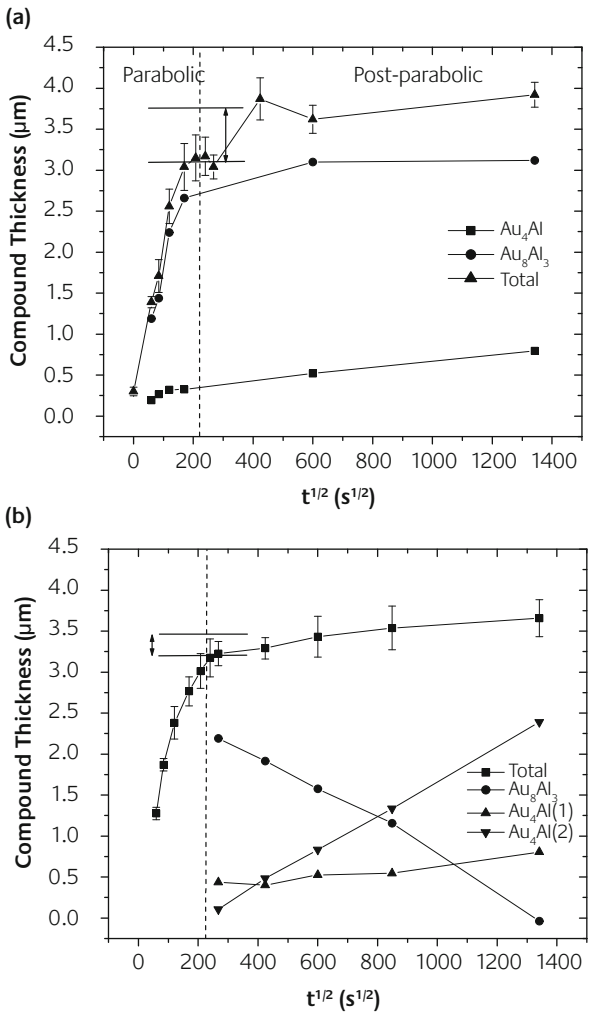

Intermetallic compound thickness plotted against the square root of time for various compounds after isothermal ageing at 175°C. (a) Wire Type A (b) Wire Type B. For both wires parabolic behaviour is observed for the total compound thickness only up to roughly $200s^{1/2}$. Lines are to guide the eye only

large enough to be measured, which is sometimes difficult during the early stages of growth. The total compound thickness (both compounds taken together) is also plotted. The graphs are divided into two timeframes, Stage I and Stage II. The first, Stage I, is approximately between $0<t^{1/2}<200s^{1/2}$ and in this time range there is a supply of Al from the bondpad for intermetallic growth. In Stage I both wire types show parabolic growth according to the Eqn. 1, where Δx is compound thickness, k_p is the parabolic growth rate (a constant) and t is time in seconds.

$$\Delta x = (2k_p t)^{\frac{1}{2}} \quad (1)$$

With both wire types, Stage I growth is essentially the same, as shown in Fig. 6(a) and Fig. 6(b). As already noted, the first compound formed is Au_8Al_3, which rapidly grows and is the dominant compound. At $t^{1/2} \approx 50s^{1/2}$ (1 hour) a very thin second phase grows in Type A wire between Au and Au_8Al_3. The phase is assumed to be the first layer of Au_4Al and although in Type B wire it appears at around the same time the phase is thinner than in the A wire, difficult to measure and is therefore not plotted in Fig.1. Therefore the parabolic growth rate constant k_p cannot be measured for the compounds in both wires and only the total compound growth constant k_p is presented in Table 2. The numerical value of k_p is in the range 0.3-1.5 x 10^{-16} m^2s^{-1}, similar in magnitude to data commonly reported for diffusion couples [19]. Intermetallic thickness is similar in both wire types at the same times although k_p for B wire is significantly smaller than Type A wire. However, the data for wire B shows some slight curvature that indicates a relatively small deviation from parabolic growth. Parabolic growth assumes that vacancy equilibrium and the curvature seen with B wire may indicate some supersaturation of vacancies. Exceptions to parabolic behaviour are known and linear kinetics may occur during the early stages of intermetallic growth [20] while exponents of greater than ½ and between 2-5 have been observed, which are attributed to several effects including change of atomic volume of diffusing species when forming intermetallics, formation of non-equilibrium defects in the growing phase and time dependent diffusivity [21].

In Stage II, defined as $t^{1/2}>200s^{1/2}$, the wires show significant differences in behaviour, as shown in Fig. 6. In Type A wire, Au_4Al (layer 1) and Au_8Al_3 remain as the major compounds under the centre of the ball and although there is no longer a supply of Al, further total compound thickening occurs between $200\leq t^{1/2}\leq 400s^{1/2}$, increasing by ≈0.8µm. The increase in thickness is ≈0.5µm for Au_8Al_3 and ≈ 0.3µm for Au_4Al(layer 1) and with very small growth rates (Table 3). Although there is some slight variation in compound thickness between $200\leq t^{1/2}\leq 400s^{1/2}$, at $t>400s^{1/2}$, a plateau is reached. Type B wire exhibits very different behaviour. The first layer of Au_4Al remains and a second layer of Au_4Al grows with parabolic time dependence between Au_4Al (layer 1) and Au_8Al_3, growing at the expense of Au_8Al_3, which as Fig. 6(b) shows, decreases in thickness as it undergoes a phase transformation to Au_4Al. In order for the transformation to occur gold must diffuse to the Au_8Al_3. Type B wire shows an overall increase in thickness of ≈0.5µm between $200\leq t^{1/2}\leq 1400s^{1/2}$, partly due to some thickening of $Au_4Al(1)$ and a steady increase in the thickness of Au_4Al (layer 2). Growth (shrinkage) rates are also very small, as shown in Table 3. In Stage II, Au_4Al (layer 2) growth is in Fig. 1(b) to be parabolic but starts at a later time t_0 and therefore thickness increases as defined in Eqn. 2, where t_0 is the time at which Au_4Al (layer 2) growth starts.

Table 3

Post-parabolic growth rates measured for the individual compound thicknesses of wire types A and B

Wire Type	Growth Rate k_p (m^2s^{-1} x 10^{-16})		
	$Au_4Al(1)$	$Au_4Al(2)$	Au_8Al_3
A	0.0008	NA	0.0012
B	0.0017	0.0198	-0.023

$$\Delta x = \left[2k_p(t - t_0)\right]^{\frac{1}{2}} \quad (2)$$

From experimental data in Fig. 1(b) the growth rate constant for the second layer of Au_4Al is $k_p = 1.98 \times 10^{-18}$ m^2s^{-1} (see Table 2) and the constant $t_0^{1/2}$ is estimated as $268s^{1/2}$ from Fig. 6(b).

A concern with all studies on intermetallic growth is mechanical strength of ballbonds. Pull strength data for each wire in Fig. 7 show that the ballbonds remain mechanically robust during ageing. Type A wire shows slightly higher pull strength than Type B.

Figure 7

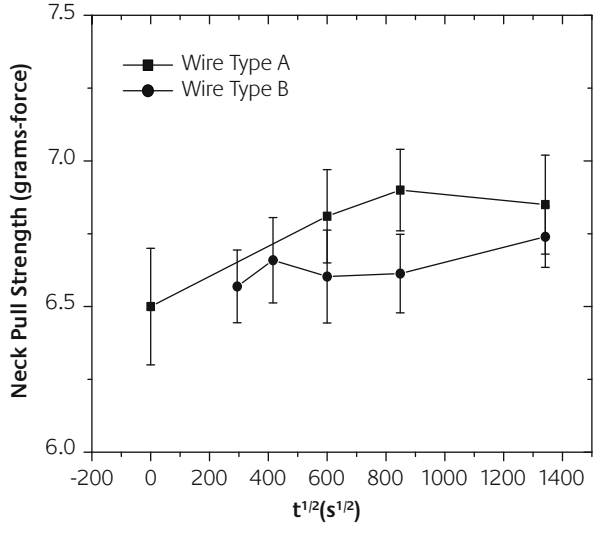

Pull strength data of wires after isothermal ageing at 175°C up to $1341s^{1/2}$ (500hrs). Lines are to guide the eye only

3.3 Chemical diffusion process in gold ballbonds on Al metallization

The previous section presents compound chemistry and the order of appearance without considering the diffusion mechanism. The diffusion mechanism is important because stoichiometry determines how Au and Al diffuse through the various compounds to interfaces. The intermetallics Au_8Al_3 and Au_4Al are stoichiometric compounds with a very narrow solubility range and diffusion of Au and Al within the compounds should occur on the sub-lattices formed by each element. The intrinsic diffusion co-efficient of each element on the respective sub–lattice within Au_8Al_3 therefore determines the speed of diffusion of an element across the compound to an interface. The speed and ease with which diffusion occurs depends on the crystal structure of the compound which in turn determines the distance between nearest neighbours on each sub-lattice. Growth rates of the same compound at each interface may therefore be different, depending on the connectivity of each sub-lattice. For example, growth of Au_8Al_3 at the wire and chip sides depends on the rate of Al and Au diffusion to each respective interface. In stoichiometric compounds, under the assumption of thermodynamic equilibrium at each interface, activity gradients drive diffusion and intermetallic growth rather than concentration gradients [22-24]. Therefore formation of Au – Al compounds may be viewed from a slightly different perspective than commonly found in gold ballbonding literature. Intermetallic growth begins from intermetallic coverage, illustrated in Fig. 8(a). During isothermal ageing, the unbonded regions of the interface fill up by lateral growth of the coverage as illustrated in Fig. 8(b), provided there are no diffusion barriers such as oxide layers. With further ageing, a thin layer of Au_8Al_3 forms and once the layer covers the whole interface, further growth requires that Au and Al diffuse through Au_8Al_3 to each interface on the respective sub-lattices, as Fig. 8(c) illustrates. As the Au_8Al_3 layer gets

Figure 8

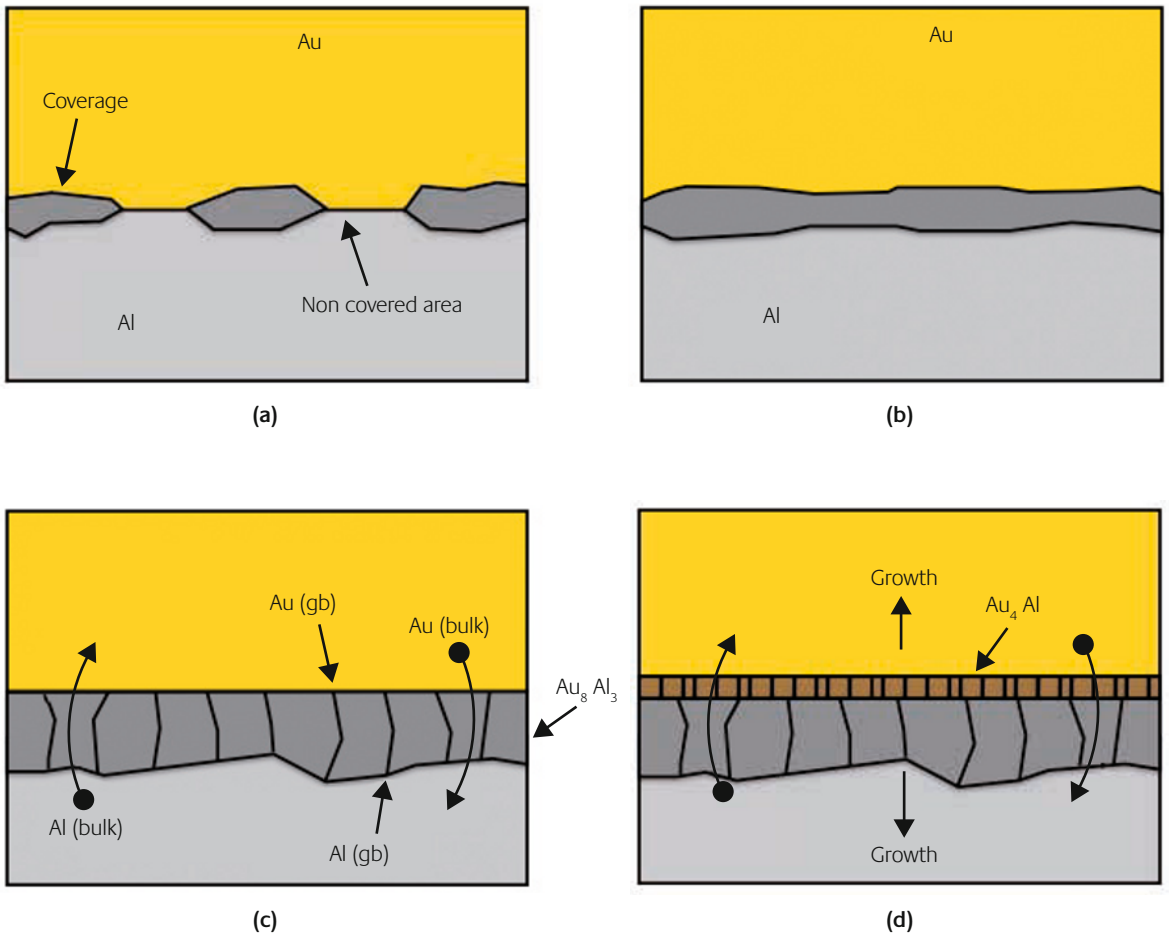

Illustrations (not to scale) of Stage I growth for A and B wire types. (a) Schematic showing the intermetallic coverage formed during ballbonding. (b) areas of the interface without intermetallic coverage fill in by lateral growth of the regions with coverage (unless there is a barrier to diffusion like an oxide) (c) With isothermal ageing, Au_8Al_3 forms first. Growth of the compound at both interfaces involves the diffusion of Au and Al. (d) After further ageing Au_4Al forms and further growth of Au_8Al_3 requires Au to diffuse across both product layers

Figure 9

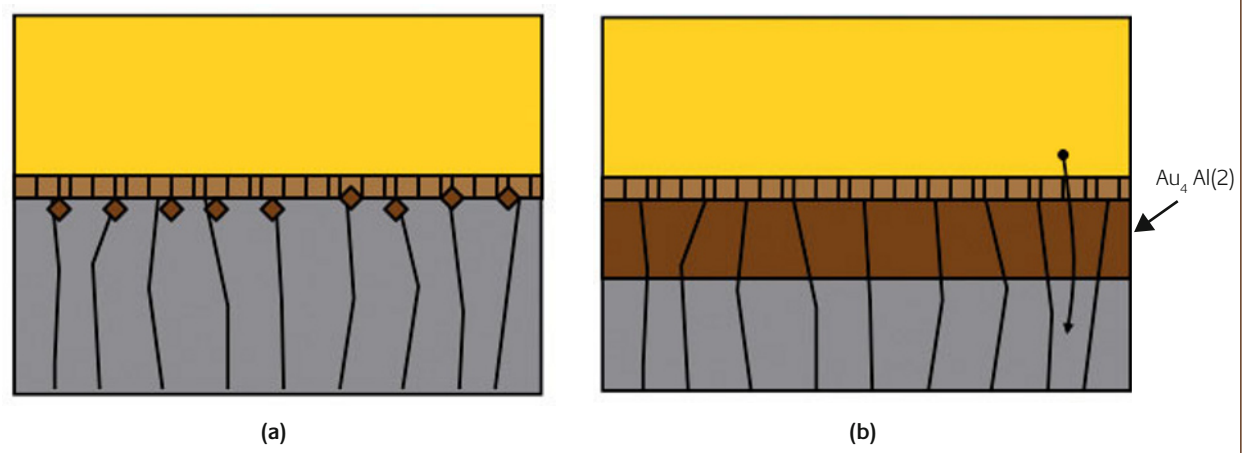

Stage II growth in Type B wire. (a) Au diffuses through $Au_4Al(1)$ to the $Au_4Al(1)$-Au_8Al_3 interface and the phase transformation starts as indicated by the diamond shapes. (b) Continued growth of $Au_4Al(2)$ requires that Au diffuses through $Au_4Al(1)$ and $Au_4Al(2)$

thicker, the number of atoms of Au and Al arriving per unit time at the Au -Au_8Al_3 and Au_8Al_3 – Al interfaces decreases (assuming constant velocity) and the growth rate of Au_8Al_3 at each interface slows down. When the growth rate of Au_8Al_3 at either interface becomes so slow that the rate of reduction of free energy becomes very small (despite Au_8Al_3 having the lowest free energy), the overall rate of decrease of system energy slows down. The rate of free energy decrease can however become faster by forming a phase that is easier to assemble with the reduced flux of atoms, and therefore grows faster even if that phase does not have the lowest free energy. Therefore, as Fig. 8(d) illustrates and as Fig. 2(a) shows, the first layer of Au_4Al forms between Au and Au_8Al_3 when there is still Al available for reaction with Au and formation of Au_8Al_3 near the chip, which suggest that the flux of Al to that interface is too small to permit growth of Au_8Al_3 at a fast enough rate. However, the continued growth of Au_8Al_3 at the Au_8Al_3 – Al interface shows the phase forms relatively easily and therefore there is a sufficiently high flux of gold through Au_8Al_3 despite the apparently complex crystallography of this compound [25]. This view is contrary to the common perception in ballbonding literature that Al always diffuses faster than Au during intermetallic growth in ballbonds. Similar observations have been reported in studies of self-diffusion in intermetallics [26, 27] that show the speed with which each element diffuses across a compound layer depends on the local structure of each respective sub-lattice. This idea has been expressed by d'Heurle et al as the 'ordered Cu_3Au rule' [28, 29], from observations that in ordered compounds, the majority element naturally diffuses more easily because the sub-lattice has greater connectivity, a concept that is widely accepted. Therefore it appears that the rates of formation of the same compound at different interfaces in gold ballbonds depend on the diffusion of each element on the respective sub-lattice.

Growth of Au_8Al_3 continues as long as Al is available in the bondpad metallization and stops when Au_8Al_3 grows to the Si chip (Fig 4(b)) with a small increase in thickness of the Au_4Al, marking the end of parabolic growth (Fig. 7). For Wire Type A, this marks the end of the major intermetallic growth process, except for some small amount of thickening in Au_4Al that appears to be a common feature amongst different wire types [30]. However, in Type B wire conversion of Au_8Al_3 to the more gold-rich Au_4Al occurs after complete consumption of Al, which can only begin by diffusion of gold from the bonding wire, through the first layer of Au_4Al to Au_8Al_3.

In addition to the bulk diffusion mechanism described above, grain boundary diffusion can also occur. The grains of the first layer of Au_4Al are narrow and columnar and grain boundary diffusion ought to contribute more to the diffusion flux than through the larger grains of Au_8Al_3. Grain boundary diffusion in intermetallics is generally not as simple as in random alloys and the concentration of component atoms at the boundary can depend on the stoichiometry in the bulk. Compounds with narrow ranges of bulk composition may therefore have unique grain boundary structures with a unique electron distribution at the boundary that may also affect interaction with impurity atoms [31]. There is no research literature on the grain boundary structure of Au – Al compounds and nothing further can be said about the effects of grain boundary structure on the interdiffusion process.

Table 4

Heats of formation of Au – Al compounds calculated using the Miedema macroscopic atom model [47] together with selected fundamental physical properties

Compound	Composition (at% Au)	ΔH^o (kJ/mol)	ΔH_f (kJ/mol at)	$\Delta H_f'$ (kJ/mol at)	Molar Mass (g)	Density (g/cm^3)	Molar Volume (cm^3)
Au	NA	NA	NA	NA	196.96*	19.3	10.19*
Au_4Al	80	-95	-19	-18.5	814.82	16.2	50.29
Au_8Al_3	72.72	-286	-26	-20	1656.62	14.9	111.18
Au_2Al	66.67	-90	-30	-19.8	420.90	13.7	30.72
AuAl	50	-74	-37	-16.3	223.94	10.7	20.92
$AuAl_2$	33.37	-93	-31	-10.2	250.92	7.5	33.46
Al	NA	NA	NA	NA	26.98*	2.69	10.0*

*J Emsley. The Elements. Cambridge University Press, 3rd Edn. 1998

3.4 Analysis of $Au_8Al_3 \rightarrow Au_4Al$ phase transformation and growth kinetics

Under the assumption that transformation of Au_8Al_3 into a second layer of Au_4Al requires diffusion of Au through the first layer of Au_4Al to Au_8Al_3 it is possible to analyze diffusion kinetics within the framework of linear irreversible thermodynamics. An assumption is that the driving force for diffusion is an activity gradient [19-21], which may be due to some effect of dopants. A further assumption is the Au – Al system with dopants and bondpad elements is quasi-binary i.e. there is no modification to the intermetallic structure. Analysis of the diffusion process begins with the assumption that the mobile species are Au and Au sub-lattice vacancies and following the steps of van Loo et al [23], Darken's equation, below, is the starting point of the analysis.

$$D_{Au} = D^*_{Au}\left[1 + \frac{\partial \ln \gamma_{Au}}{\partial \ln N_{Au}}\right] = D^*_{Au}\left[\frac{\partial \ln a_{Au}}{\partial \ln N_{Au}}\right] \qquad (3)$$

In Eqn. (3), D_{Au} is the chemical diffusion coefficient, γ is the activity co-efficient, a the concentration, N the mol fraction. D_{Au}^* is the tracer or self-diffusion diffusion co-efficient of Au in the phase Au_4Al (layer 2) at the given temperature that represents the mobility of a species in a solid phase in the absence of thermodynamic effects. The tracer diffusion coefficient D_{Au}^* is a constant, i.e. it is a material constant for a given composition at a given temperature and the thermodynamic factor in square brackets takes account of the conditions at the interfaces (boundaries) with other phases that affect the diffusion rate. Ideally, D_{Au}^* would be experimentally measured in the different Au – Al compounds over a range of temperatures. The flux of Au through Au_4Al (layer 1) is written as

$$J_{Au} = -D^*_{Au}\frac{\partial c_{Au}}{\partial x}\left[\frac{\partial \ln a_{Au}}{\partial \ln N_{Au}}\right] \qquad (4)$$

Where c_{Au} is the concentration of Au in the compound in mol/m^3. However, assuming Au_4Al to be a stoichiometric compound, there is no concentration gradient. Therefore, write

$$dc_{Au} = d\left(\frac{N_{Au}^{Au_4Al(2)}}{V_M^{Au_4Al(2)}}\right) \qquad (5)$$

Assuming constant molar volume and inserting Eqn. 5 into Eqn. 4, the following expression is found

$$J_{Au}\Delta x = -D^*_{Au}\left(\frac{N_{Au}^{Au_4Al(2)}}{V_M^{Au_4Al(2)}}\right)\int_{a'_{Au}}^{a''_{Au}} d\ln a_{Au} \qquad (6)$$

In Eqn. (6) N_{Au} is number of moles of Au in the compound, $V_M^{Au4Al(2)}$ is the molar volume of the growing compound, a_{Au} is the activity of Au at interfaces I (Au – $Au_4Al(1)$) and II ($Au_4Al(2)$ – Au_8Al_3). On integrating, Eqn. (6) becomes

$$J_{Au}\Delta x = -D^*_{Au}\left(\frac{N_{Au}^{Au_4Al(2)}}{V_M^{Au_4Al(2)}}\right)\left[\ln a''_{Au} - \ln a'_{Au}\right] \qquad (7)$$

An important point is that D_{Au}^* is a constant for phase of known composition but varies with temperature but it is not a function of the activity gradient across the Au_4Al (layer 2) compound. Expressions for the chemical potential of Au at each interface are

$$\mu'_{Au} = \mu^0_{Au} + RT\ln a'_{Au} = \mu^0_{Au} + RT\ln \gamma'_{Au}N'_{Au}$$
$$\mu''_{Au} = \mu^0_{Au} + RT\ln a''_{Au} = \mu^0_{Au} + RT\ln \gamma''_{Au}N''_{Au} \qquad (8)$$

In Eqn. 8, μ_{Au}^0 is the chemical potential of pure Au, γ_{Au}^i is the activity co-efficient of Au at interface 1 or 2, and N_{Au}^i is the fraction of Au at interface 1 or 2.

The difference in chemical potential of Au between interfaces II and I is

$$\Delta\mu_{Au} = \mu^{II}_{Au} - \mu^{I}_{Au} = RT\left[\ln a^{II}_{Au} - \ln a^{I}_{Au}\right] = \Delta_R G^0_{Au} \quad (9)$$

Where $\Delta_R G_{Au}{}^0$ is the free energy of reaction per moving Au atom. Assume

$$\Delta_R G^0_{Au} = \Delta_R H^0_{Au} - T\Delta_R S^0_{Au} \approx \Delta_R H^0_{Au} \quad (10)$$

Where $\Delta_R H_{Au}{}^0$ and $\Delta_R S_{Au}{}^0$ are the free enthalpy and entropy of reaction per moving Au atom respectively. Then Eqn. (5) can be written as

$$J_{Au}\Delta x = -D^*_{Au}\left(\frac{N^{Au_4Al(2)}_{Au}}{V^{Au_4Al(2)}_M}\right)\frac{\Delta_R H^0_{Au}}{RT} \quad (11)$$

The growth rate of the compound can be written as

$$\frac{dx}{dt} = \frac{k_p}{\Delta x} = J_{Au}V_m^{Au4Al(2)}n_{Au_4Al(2)} \quad (12)$$

In Eqn. (10), $n_{Au4Al(2)}$ is the number of moles of product formed per mole of Au diffusing across the product layer ($n_{Au4Al(2)}$ is a dimensionless term). Expressions for $J_{Au}V_m{}^{Au4Al(2)}\Delta x$ obtained from (5) and (9) can be equated and rearranged to show

$$D^*_{Au} = -\frac{k_p RT}{n_{Au_4Al(2)}N^{Au_4Al(2)}_{Au}\Delta_R H^0_{Au}} \quad (13)$$

In principle, a simple estimate of the thermodynamic factor can also be made as follows:

$$x^2 = 2D_{Au}t = 2D^*_{Au}t\left[\frac{\partial \ln a_{Au}}{\partial \ln N_{Au}}\right] = 2k_p t \quad (14)$$

From this equation the thermodynamic factor can be written as

$$\left[\frac{\partial \ln a_{Au}}{\partial \ln N_{Au}}\right] = \frac{k_p}{D^*_{Au}} = -\frac{n_{Au_4Al(2)}N^{Au_4Al(2)}_{Au}\Delta_R H^0_{Au}}{RT} \quad (15)$$

Where $n_{Au4Al(2)}$ is the number of moles of the second layer of Au_4Al compound formed per mole of diffusing gold. The term $N_{Au}{}^{Au4Al(2)}$ is 4/5, the mole fraction of gold in Au_4Al (layer 2). The thermodynamic factor depends on the heat of reaction, which as it becomes more negative results in a larger activity gradient. An estimate of the thermodynamic factor requires knowledge of the specific reaction that results in the formation of Au_4Al(layer 2), but the reaction is unknown and so therefore is $A\Delta_R H^0{}_{Au}$. A simple reaction involving only diffusion of Au can be written (1/4) Au_8Al_3 + Au ⟶ (3/4) Au_4Al, but this is simply an equation with a very low free energy change, making it highly unlikely to occur and lacking physical basis. The microscopic mechanism behind the conversion is more complex, probably involving creation of an activity gradient by interactions between dopants or bondpad elements and gold in Au_8Al_3. Therefore $n_{Au4Al(2)}$, the number of moles of the second layer of Au_4Al formed per mole of diffusing gold atoms is unknown. However, by using hypothetical values of $n_{Au4Al(2)}$ and $\Delta_R H^0{}_{Au}$ and examining the diffusion co-efficient and activity gradients it is possible to make some hypotheses about the diffusion reaction process. Table 5 shows values of D_{Au}, $D_{Au}{}^*$ and the thermodynamic factor calculated with various assumed values of $A\Delta_R H_{Au}{}^0$. As expected D_{Au} is the same regardless of the assumed values while $D_{Au}{}^*$ and the thermodynamic factor vary. The thermodynamic factor becomes larger in direct proportion to the free energy change for the phase transformation. The reaction therefore becomes more probable as $\Delta_R H_{Au}{}^0$ becomes larger (more negative).

Table 5

Thermodynamic factor estimates using the reaction equation and hypothetical values of $\Delta_R H_{Au}{}^0$

Hypothetical $\Delta_R H_{Au}{}^0$ (kJ/mol)	n_{Au4Al}	$D_{Au}{}^*$ (m^2s^{-1} x 10^{-18})	Thermodynamic Factor $\frac{\partial \ln a_{AU}}{\partial \ln N_{AU}}$	D_{Au} (m^2s^{-1} x 10^{-18})
-2.5	0.5	7.37	0.27	1.98
-5		3.69	0.54	
-10		1.84	1.07	
-20		***0.92***	***2.15***	
-40		***0.46***	***4.3***	
-2.5	***1***	3.69	0.54	
-5		1.84	1.07	
-10		***0.92***	***2.15***	
-20		***0.46***	***4.30***	
-40		***0.23***	***8.59***	

Figure 10

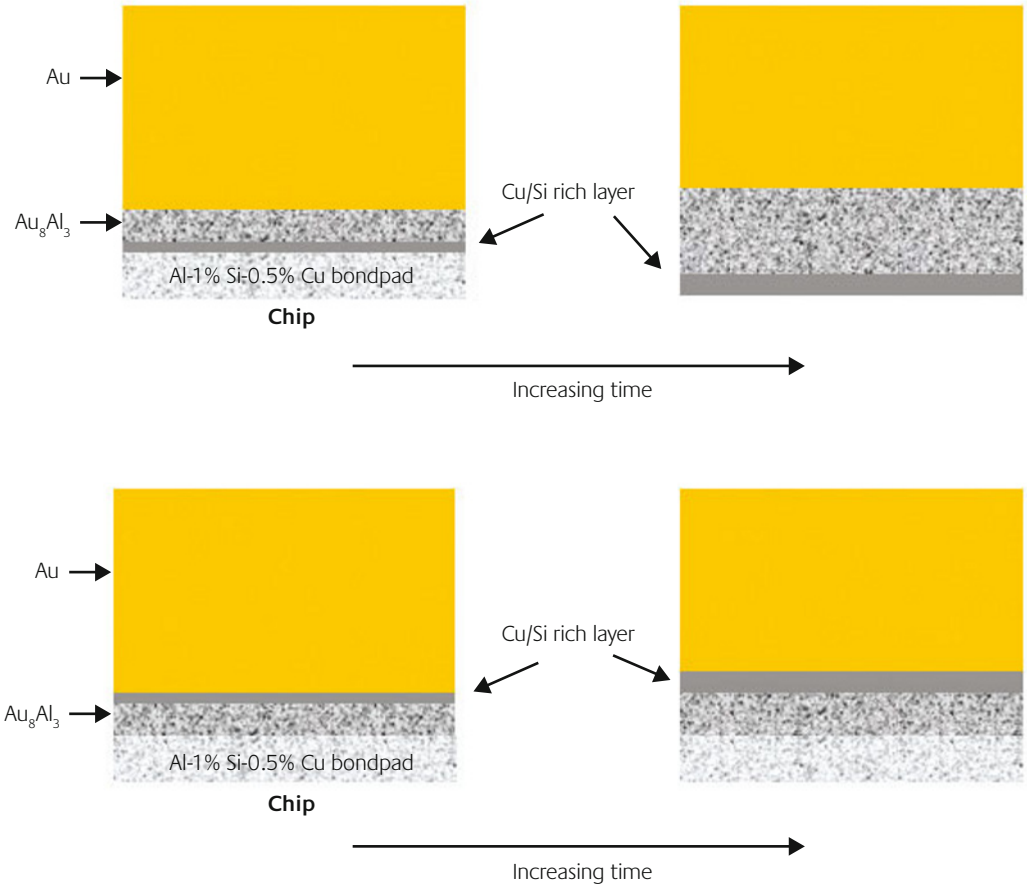

Illustration of what might happen if Si and/or Cu come out of solution and form distinct layers as Au_8Al_3 grows. (a) thin Cu/Si rich layer may appear between Au_8Al_3 and Al, forming a diffusion barrier and slowing down growth of Au_8Al_3 (b) similar situation with Cu/Si rich layer between Au and Au_8Al_3. With increasing time the amount of Cu/Si should increase as more Al is consumed and a thicker Cu/Si layer forms

4 Discussion

Prior to consumption of aluminium in the bondpad, intermetallic growth with both wire types is similar in that the sequence of compound formation is the same and occurs with parabolic growth dependence that demonstrates diffusion controlled growth. Differences in chemistry appear to have no effect during parabolic growth. The conversion of Au_8Al_3 into the more gold-rich Au_4Al only with Type B wire after parabolic growth stops suggests an effect of wire chemistry. The phase change requires a source of gold, which is assumed to come from diffusion of Au from the wire through Au_4Al to Au_8Al_3, where a reaction occurs with Au_8Al_3. Assuming the compounds are stoichiometric, the diffusion analysis presented earlier suggests the driving force for diffusion is a gold activity gradient and therefore gold activity at interface II is less than at interface I. A reduction in Au activity at interface II is speculated to be caused by attractive interactions between dopants, Cu and Si and Au in Au_8Al_3.

To understand this hypothesis it is necessary to understand the meaning of activity. Activity in alloys can be measured as the vapour pressure of each element above the surface of an alloy or compound over the whole composition range between pure elements [32]. In ideal solutions, in which interactions between elements are ignored, activity $a = \gamma N$ is equal to the fraction of each element in the alloy (see Eqn. 6). In alloys or compounds where elements are attracted to one another the enthalpy of mixing is negative and the activity co-efficient γ is less than one. Elements that prefer their own kind tend to cluster and form multiphase materials with $\gamma > 1$. Activity at interfaces appears a little more difficult to visualize than at surfaces but structure of a binary phase in an interface may have a specific crystallographic structure that exposes one or other element and affects the surface concentration and therefore the activity of the components at an interface. If dopants or other additional minor elements present in a quasi-binary alloy segregate to interfaces, attractive interactions can potentially reduce the overall free energy. For example, in segregating to an interface, a minor element may lower the overall system free energy by bonding

with alloy elements in one of the bulk phases. In the case of the Au_8Al_3 to Au_4Al phase transformation, which occurs only after relatively long times, the hypothesis is that dopants, Cu and/or Si act to reduce gold activity in Au_8Al_3, giving rise to an activity gradient.

The problem with this hypothesis is that experimental data in this study does not permit a direct understanding of how the additional elements Cu, Si and dopants might behave. It is possible however, to suggest how Cu and Si behave in both wire types during parabolic growth because both elements are present in far larger amounts than dopants. For the sake of argument, assume that Cu and Si are totally insoluble in Au – Al intermetallic compounds. During the early stages of intermetallic growth with both wire types only Au_8Al_3 is present and as it grows thicker and reaches the Si chip, Cu and Si from the Al bondpad will not be permitted to become part of the intermetallic. Therefore the local concentration of Cu and Si in the remaining Al increases, eventually forming a Cu/Si rich layer illustrated schematically in Fig. 10. This layer would also prevent or slow down the growth of Au_8Al_3 perhaps preventing contacting with the chip if the layer forms between Au_8Al_3 and Al. Alternatively, the layer would also act as a diffusion barrier if it forms between Au and Au_8Al_3. Similar behaviour is seen to 99.9% Au wires with high Pd content on Al metallization; Pd is not soluble in the Au – Al intermetallics and a Pd rich layer is seen between the wire and the intermetallic [33]. However, a Cu/Si rich layer is not seen and therefore Cu and Si must be distributed in some manner within the intermetallic compound. If Cu and Si have some solubility in Au_8Al_3, they may substitute for Au or Al on the lattice, perhaps also segregating to grain boundaries. If Cu and Si become soluble to some extent in the intermetallic, the diffusion process leading to the formation of Au_8Al_3 should be different. Assuming the Au_8Al_3 compound is stoichiometric with a narrow stability range, the much lower concentrations of Cu and/or Si cannot form separate lattices and presumably substitute for either Au or Al. Growth of Au_8Al_3 requires diffusion of Au and Al to opposite interfaces via the lattice with an additional path via grain boundaries. If Cu and/or Si show a preference for one of the lattices (Au or Al), presumably, diffusion of Cu and Si is restricted to that lattice. Philofsky [13] reports that Si forms $AuSiAl_4$ compound but neither Si nor Cu were detectable with standard EDX spot or mapping analysis. It is therefore impossible to know how Cu and Si distribute throughout Au_8Al_3 without using more sophisticated experimental tools but both elements must be part of the compound, either on the lattice or segregated at grain boundaries or both. Assuming that Cu and Si are part of the first compound that grows, Au_8Al_3, growth of Au_4Al (layer 1), which starts when Au_8Al_3 reaches a critical thickness, must occur by the usual mechanism of diffusion of Al through Au_8Al_3 and Au_4Al (layer 1) to the Au – Au_4Al (layer 1) interface. It is uncertain if Cu and Si diffuse into Au_4Al (layer 1) and substitute for Au or Al and because the compound does not change with either wire type, effects of Cu and Si on Au_4Al(layer 1) are assumed negligible and are not further discussed.

Substitution of Cu and Si in for Au or Al in Au_8Al_3 and segregation to grain boundaries is expected to be the same regardless of wire type but the phase transformation of Au_8Al_3 to Au_4Al only occurs with Type B wire. The only difference between devices bonded with A and B wires is chemical nature of the dopants and therefore the phase transformation is assumed to be a direct consequence of different dopants or at least the dopants play a major role in driving the phase transformation. The extremely small amount of dopants in comparison with Cu and Si makes it unlikely that they become part of the intermetallic structure but it is conceivable that they segregate to grain boundaries within Au_8Al_3, interact with Au at the interfaces and cause a reduction in Au activity. The tendency of an element to segregate is related to the solubility of that element in the host metal or compound and grain boundary structure also affects segregation behaviour, grain boundaries with more dislocations cores usually accommodating segregated elements quite readily because of the larger available volume. Many metallurgical studies suggest that impurities can interact extensively with the host metals in alloys and can attract or repel other impurities or elements, potentially affecting the thermodynamic activity [34-38]. In addition, the same elements may segregate to grain boundaries and interfaces, particularly when the solubility of the elements in the host is severely limited [39] and elements may co-segregate and interact at the same time. Segregation reduces interfacial and grain boundary energy and segregated elements can increase or decrease cohesion of grain boundaries through bonding interactions with the solvent. It is possible that dopants segregate to the grain boundaries of Au_8Al_3 during initial growth and remain there as Au_4Al grows. Clearly however, the exact mechanism remains unknown and it can only be assumed that dopants (perhaps interacting with Cu and/or Si) cause a reduction in activity or more specifically, activity co-efficient, at the Au_4Al(layer 1) – Au_8Al_3 interface, which provides a thermodynamic driving force for diffusion of Au and the phase transition. Investigations of the effects of impurities on intermetallic growth shows that activity of diffusing elements may reduce or increase and result in a reduction/increase of intermetallic thickness [34, 35].

Although activity and activity gradient is not measurable in this study it is possible to calculate the thermodynamic factor across the growing new phase Au_4Al (layer 2) by assuming numerical values for the term $n_{Au4Al}\ \Delta_R H_{Au}{}^0$. The results of the calculation are in Table 5, which shows the assumed number of moles of product, the assumed heat of reaction, the calculated intrinsic diffusion coefficient and the thermodynamic factor. The significance of the intrinsic diffusion co-efficient $D_{Au}{}^*$ is that it is the self-diffusivity, tracer diffusion co-efficient or mobility of Au in the homogeneous

Au_4Al (layer 2) in the absence of thermodynamic influences [40, 41]. The diffusion coefficient of Au, D_{Au} is the diffusion coefficient of Au in the presence of thermodynamic effects i.e. interactions between components undergoing mixing or reaction. The calculated values of the thermodynamic factor vary from less than one to much greater than one, depending on the assumed number of moles of Au_4Al (layer 2) produced and the accompanying reduction of free energy measured by $\Delta_R H_{Au}{}^0$. The thermodynamic factor is interpreted as an indicator of the departure of concentrated solutions from ideal behaviour and therefore it is a measure of the extent of interaction between components of a solution [42]. In chemical diffusion studies, a high degree of interaction between the components of a growing phase affects the diffusion of each element across the product layer and therefore intermediate phases and intermetallic compound layers often have large thermodynamic factors compared with random alloys [43]. Generally the thermodynamic factor should be greater than zero for phase stability in regular solutions [44] and according to Baird [24] a low value of $\delta\log a / \delta\log N$ for an intermediate phase indicates marginal stability with respect to adjoining phases. Baird cites Cu-Zn phases as an example, where $\delta\log a_{Zn} / \delta\log N_{Zn}$ can be quite large for β (4) and γ (19) phases. Therefore the occurrence of the phase transformation Au_8Al_3 to Au_4Al (layer 2) implies high stability for the new phase and a sizeable thermodynamic factor. In addition, the free energy change for the phase transformation plays an important role and clearly the larger (more negative) the free energy change, the more likely the transformation. Although it is impossible to know the reaction details, making the calculated data in Table 2 entirely speculative, physical intuition leads to the conclusion that the thermodynamic factor must be larger than one and that the heat of reaction needs to be of realistic proportions i.e. a heat of reaction of -1kJ/mol is unlikely to result in a reaction. The intrinsic diffusion co-efficient $D_{Au}{}^* < D_{Au}$ is also a requirement because the thermodynamic factor represents the contribution of thermodynamic forces to the enhancement of $D_{Au}{}^*$. A tentative conclusion is that the heat of reaction should be reasonably large, in the range 10-20 kJ/mol or more.

5 Summary and conclusions

Two wires of different chemistry, Type A and Type B, ballbonded to the identical bondpad metallization grow the same intermetallics during parabolic growth but after extended ageing Au_8Al_3 undergoes a phase transformation into a compound, which, from EDX analysis, has the same composition as Au_4Al (layer 1). The occurrence of the phase transformation only in Type B wire only is attributed to dopants in the wire that may interact with other dopants and/or with bondpad elements and reduce the activity of Au in Au_8Al_3. The resulting activity gradient is proposed to drive the diffusion of gold from the wire into the Au_8Al_3, causing the transformation of Au_8Al_3 into Au_4Al (layer 2). The reliability of ballbonds made with Type B wire, measured from the pull strength stability over time, is not affected by the phase transformation and it should not be a concern for package reliability provided the process parameters are correctly optimized.

Acknowledgements

The authors wish to acknowledge the discussions with Dr. Richard Blish, Spansion Senior Fellow, 915 DeGuigne, MS 33, PO Box 3453, Sunnyvale, CA 94088-3453, USA.

About the authors

Dr. Christopher Breach is a consultant at ProMat Consultants based in Singapore. He was formerly Director of R&D for Kulicke & Soffa bonding wire in Singapore. He was also a research scientist for Singapore Institute of Manufacturing Technology researching inkjet/microjet process applications and materials development in flexible and macro-electronics and providing expertise in a wide range of physical and chemical characterization techniques. He holds a PhD in physics & physical chemistry of materials (sponsored by the Defence Research Agency) from Brunel University, London. His postdoctoral research was sponsored by ICI at the Department of Physics, Cavendish Laboratory, University of Cambridge on the relationship between interdiffusion in polymers (reptation) and the physics of bi-material fracture. He is a Chartered Scientist, Chartered Physicist, Professional Member of the Institute of Physics, member of The Institute of Electrical and Electronics Engineers (IEEE) and the Materials Research Society (MRS).

Mr. Frank Wulff is Manager for Materials Development & Characterization at Kulicke & Soffa's bonding wire R&D facility in Singapore and has been with K&S for 10 years. Prior to joining Kulicke & Soffa, Mr. Wulff worked in industrial failure analysis and materials characterization for CEM Research Institute (Now Fraunhofer) for 6 years. His research interests include materials design, characterization, materials processing and reliability.

References

1 G. Harman. Wire bonding in microelectronics: materials, processes, reliability and yield. McGraw-Hill electronics packaging and interconnection series. 2nd Edn. 1997

2 C.D. Breach, F. Wulff. *Microelectronics Reliability* **44** (2004) 973

3 N. Noolu, N. Murdheshwar, K. Ely, J. Lippold, W. Baeslack. *Journal of Electronic Materials* **33** (2004); 340

4 G.Y. Jang, J.G. Duh, H. Takahashi, D. Su. *Journal of Electronic Materials* **35** (2006); 323

5 P.D. Ngo, Chapter 4 in Failure Analysis of Integrated Circuits: Tools & Techniques, Edited by L.C. Wagner. Springer –Verlag Series in Engineering & Computer Science (1999)

6 R.C. Blish, S. Li, H. Kinoshita, S. Morgan, A. Myers. IEEE 44th Ann. Reliability Physics Symposium, San Jose, 233 (2006)

7 V. Koeninger, H.H. Uchida, E. Fromm. IEEE Trans. Comp. Packg. And Manfg. *Tech.-Part A* **18(4)** (1995) 835

8 T. Uno, K. Tatsumi, Y. Ohno. *Proc. ASME/ISME Advances in Electr. Packaging EEP* **1-2** (1992)

9 C.D. Breach, F. Wulff, K. Dittmer, M. Garnier, V. Boillot and C.W. Tok. Proceedings of Semicon Technical Symposium S2, p78-87 May 6th Singapore (2004)

10 Y.H. Chew, C.C. Wong, C.D. Breach, F. Wulff, T.T. Lin and C.B. He. Proceedings of ICMAT 2005 Symposium H

11 Y.H. Chew, C.C. Wong, C.D. Breach, F. Wulff, C.I. Pang and Saraswati. *Thin Solid Films* 462-463 (2004) 346

12 J.G.M. Becht, F.J.J. van Loo, R. Metselaar. *Reactivity of Solids* **6** (1988) 45

13 E. Philofsky. *Solid State Electronics* **13** (1970) 1391

14 N. Noolu, K. Klossner, K. Ely, J. Lippold, N. Murdeshwar, W. Baeslack. Proc. SMTA Conf. on Emerging Technologies, 11th Jan. 2000

15 H.S. Chang, K.C. Hsieh, T. Martens, A. Yang. *IEEE Transactions on Comp. and Packgg. Techn.* **27** (2004) 155

16 R. Pretorius, T.K. Marais, C. Theron. *Mater. Sci. Eng.* **10** (1993) 1

17 G. Majni, C. Nobili, G. Ottaviani, M. Costato. *J. Appl. Phys.* **52(6)** (1981) 4047

18 F. Wulff, C.D. Breach, Saraswati, K. Dittmer, M. Garnier. Proc. Semicon Technical Symposium 2005, Session S2, May 6th, Singapore

19 V.I. Dybkov. Reaction Diffusion and Solid State Chemical Kinetics. IPMS Publications Kyiv 2002

20 T. Laurila, V. Vuorine, J.K. Kivilahti. *Materials Science and Engineering* **R49** (2004) 1

21 G. Ghosh. *Acta Materialia* **48** (200) 3719

22 C. Wagner. *Acta Metallurgica* **17** (1969) 99

23 F.J.J. van Loo, M.R. Rijnders, K.J. Rönka, J.H. Gülpen, A.A. Kodentsov. *Solid State Ionics* **95** (1997) 95

24 J.D. Baird. *J. Nucl. Energy Part A: Reactor Science* **11** (1960) 81

25 K.J. Range, H. Buechler. *J. Alloys and Compounds* **154** (1989) 251

26 C. Herzig, S. Divinsky. Chapter 4 in Diffusion Processes in Advanced Technological Materials, Ed. D. Gupta. William Andrew Inc. 2005

27 F.M. d'Heurle, R. Ghez. *Thin Solid Films* **215** (1992) 26

28 F.M. d'Heurle, P. Gas, J. Philbert. *Solid State Phenomena* **41** (1995) 93

29 F.M. d'Heurle, C. Lavoie, P. Gas, J. Philibert. Chapter 6 in Diffusion Processes in Advanced Technological Materials, Ed. D. Gupta. William Andrew Inc. 2005

30 C.D. Breach, F.W. Wulff. Unpublished

31 T. Takasugi. Chapter 7 of Basic Mechanical Properties and Lattice Defects of Intermetallic Compounds, Ed. J.H. Westbrook and R.L. Fleischer (1995)

32 O. Kubaschewski, C.B. Alcock, P.J. Spencer. *Materials Thermochemistry*, 6th Edn., Pergamon Press 1993

33 G.Y. Jang, J.G. Duh, H. Takahashi, D. Su. *Journal of Electronic Materials* **35** (2006); 323

34 M.V. Akdeniz, A.O Mekhrabov. *Acta Materialia* **46** (1998) 1185

35 A.O. Mekhrabov, M.V. Akdeniz. *Acta Materialia* **47** (1999) 2067

36 M. Sternik, K. Krolas. *Phys. Rev.* **B 40** (1983) 4171

37 A.Z. Hrynkiewicz, K. Krolas. *Phys Rev.* **B 28** (1983) 1864

38 J.A. Alonso, T.E. Cranshaw, N.H. March. *J. Phys. Chem. Solids* **46** (1985) 1147

39 H. Wise, J. Oudar. Chapter 10 in Material Concepts in Surface Reactivity and Catalysis. Dover Publications (2001)

40 I.V. Belova, G.E. Murch. *Journal of Physics and Chemistry of Solids* **60** (1999) 2023

41 N. Karpe, J.P. Krog, J. Bøttiger, N.G. Chechenin, R.E. Somekh, A.L. Greer. *Acta Metall. Mater.* **43** (1995) 551

42 H.G. Lee. Chemical Thermodynamics for Metals and Materials. World Scientific (1999)

43 T. Ikeda, H. Nakamura, M. Koiwa. *Acta Mater.* **46** (1998) 6605

44 A.R. Allnatt, A.B. Lidiard. Atomic Transport in Solids. Cambridge University Press (1993)